

Published in final edited form as:

Cell Calcium. 2013 March ; 53(3): 187–194. doi:10.1016/j.ceca.2012.11.013.

Calcium entry via TRPC1 channels activates chloride currents in human glioma cells

Vishnu Anand Cuddapah, Kathryn L. Turner, and Harald Sontheimer

Department of Neurobiology and Center for Glial Biology in Medicine, University of Alabama at Birmingham, Birmingham, Alabama

Abstract

Malignant gliomas are highly-invasive brain cancers that carry a dismal prognosis. Recent studies indicate that Cl^- channels facilitate glioma cell invasion by promoting hydrodynamic cell shape and volume changes. Here we asked how Cl^- channels are regulated in the context of migration. Using patch-clamp recordings we show Cl^- currents are activated by physiological increases of $[\text{Ca}^{2+}]_i$ to 65 and 180 nM. Cl^- currents appear to be mediated by CIC-3, a voltage-gated, CaMKII-regulated Cl^- channel highly expressed by glioma cells. CIC-3 channels colocalized with TRPC1 on caveolar lipid rafts on glioma cell processes. Using perforated-patch electrophysiological recordings, we demonstrate that inducible knockdown of TRPC1 expression with shRNA significantly inhibited glioma Cl^- currents in a Ca^{2+} -dependent fashion, placing Cl^- channels under the regulation of Ca^{2+} entry via TRPC1. In chemotaxis assays epidermal growth factor (EGF)-induced invasion was inhibited by TRPC1 knockdown to the same extent as pharmacological block of Cl^- channels. Thus endogenous glioma Cl^- channels are regulated by TRPC1. Cl^- channels could be an important downstream target of TRPC1 in many other cells types, coupling elevations in $[\text{Ca}^{2+}]_i$ to the shape and volume changes associated with migrating cells.

Keywords

Cl^- channels; TRP channels; TRPC1; Glioma; glioblastoma; Migration; EGF; CIC-3

1. Introduction

Malignant gliomas are the most common and deadly form of primary brain cancer affecting adults. These cancers are typified by an elevated mitotic index and robust invasiveness. The invasiveness is facilitated by ion channels, which allow cellular shape and volume changes

© 2012 Elsevier Ltd. All rights reserved.

Corresponding author: Harald Sontheimer, PhD, 1719 6th Avenue South, CIRC 410, Birmingham, AL 35294, sontheimer@uab.edu.

Publisher's Disclaimer: This is a PDF file of an unedited manuscript that has been accepted for publication. As a service to our customers we are providing this early version of the manuscript. The manuscript will undergo copyediting, typesetting, and review of the resulting proof before it is published in its final citable form. Please note that during the production process errors may be discovered which could affect the content, and all legal disclaimers that apply to the journal pertain.

Conflict of Interest Statement:

We wish to confirm that there are no known conflicts of interest associated with this publication and there has been no significant financial support for this work that could have influenced its outcome.

Co-author Approval Statement:

We confirm that the manuscript has been read and approved by all named authors and that there are no other persons who satisfied the criteria for authorship but are not listed. We further confirm that the order of authors listed in the manuscript has been approved by all of us.

during migration, allowing cells to squeeze through narrow extracellular spaces. Ion channels control cellular shape and volume by moving ions, which are osmolytes, through the plasma membrane, osmotically drawing water across the cell membrane [1]. Thus, ion channels, by allowing hydrodynamic volume changes, facilitate cell migration. In glioma cells, several of the ion channels responsible for these processes have been identified and include Ca^{2+} -activated K^+ channels [2] and voltage-activated Cl^- channels/transporters [3].

Members of the CIC family of voltage-activated Cl^- channels/transporters endogenously expressed by glioma cells include CIC-2, -3, and -5 [4]. Of these channels, CIC-3 is expressed on the plasma membrane, facilitates volume and shape changes, and promotes glioma migration [3;5]. While CIC-3 seems to play an important role in migration, little is known about how CIC-3 becomes activated. We recently demonstrated that CIC-3 can be phosphorylated by Ca^{2+} /calmodulin-dependent protein kinase II (CaMKII) in human glioma cells [3] thereby coupling changes in $[\text{Ca}^{2+}]_i$ to changes in Cl^- channel activity. Upon phosphorylation, CIC-3 currents increase 3-fold, and inhibition of CIC-3 phosphorylation significantly reduces glioma cell migration [3]. Given that glioma Cl^- channels are regulated by a Ca^{2+} -sensitive kinase, the goals of the present study were to (1) determine if elevations in $[\text{Ca}^{2+}]_i$ are sufficient to increase Cl^- conductance, and (2) identify a physiological source for this Ca^{2+} .

A potential source for Ca^{2+} in glioma cells includes transient receptor potential canonical (TRPC) channels, non-selective cation channels permeable to Na^+ , K^+ , Mg^{2+} , and Ca^{2+} . Gliomas express TRPC-1, -3, and -5, which give rise to currents blocked by GdCl_3 , 2-APB, or SKF96365 [6]. TRPC1 plays a role in store-operated Ca^{2+} entry [7] and regulates EGF-induced chemotaxis in glioma cells [8]. Hence we ask whether TRPC1 is a source for Ca^{2+} to activate Cl^- channels in glioma cells.

Using inducibly-expressed TRPC1 shRNA, we find that Ca^{2+} entry through TRPC1 activates glioma Cl^- channels. We show that Cl^- channels are regulated by physiologically relevant changes in $[\text{Ca}^{2+}]_i$, i.e. between 0–180 nM. Such $[\text{Ca}^{2+}]_i$ changes occur in response to TRPC1 activity, e.g. during EGF-stimulated chemotaxis. Consistent with this we find prominent colocalization of CIC-3 and TRPC1 in caveolar lipid rafts on the processes of glioma cells. This interaction appears to be functionally relevant during EGF-induced chemotaxis.

2. Methods

2.1 Cell culture

D54 human glioma cells were derived from a World Health Organization grade IV glioblastoma and gifted to us by Dr. D. Bigner (Duke University, Durham, NC). D54 cells were maintained in Dulbecco's modified Eagle's medium/F-12 (DMEM-F/12), supplemented with 2 mM glutamine and 7% fetal bovine serum (Hyclone, Logan, UT). Cells were incubated in a humidified chamber at 37 °C and 10% CO_2 . Reagents were purchased from Sigma-Aldrich unless otherwise noted.

2.2 Electrophysiology

Whole-cell patch clamp recordings were performed on D54 glioma cells after 2–4 days in culture. Patch pipettes were pulled from thin-walled borosilicate glass (TW150F-4, World Precision Instruments, Sarasota, FL) for a final resistance of 3–5 M Ω with an upright puller (PP-830, Narashige Instruments, Tokyo, Japan). Recordings were collected with an Axopatch 200A amplifier and digitized on-line at 10 kHz and low-pass filtered at 1 kHz using a Digidata 1322A digitizer (Molecular Devices, Sunnyvale, CA). pClamp 8 software was used to acquire and store the data. Cells in which the series resistance was > 12 M Ω

were omitted, and series resistance was compensated to 80%. Standard bath and pipette solutions were used as previously described [3]. $[Ca^{2+}]_i$ was calculated with the Maxchelator program (Ca-Mg-ATP-EGTA Calculator v1.0 using constants from NIST database #46 v8).

For perforated-patch recordings, non-confluent cells cultured for 4–5 days in doxycycline or vehicle were used. Cells with series resistances up to 25 M Ω (with 80% compensation) and resting membrane potential -20 mV were used for experiments. Amphotericin B was included in the pipette solution at 240 μ g/mL, kept on ice, and used for a maximum of 4 hours after dilution. Alexa Fluor 488 hydrazide sodium salt (Invitrogen, Eugene, OR) was also included in the pipette solution at 4 μ g/mL to ensure the perforated-patch configuration was intact. If Alexa 488 filled the cell, the experiment was excluded. NPPB was applied at 200 μ M to block Cl $^-$ channels. 2-APB was applied at 100 μ M to block TRP channels. All recordings were performed in 2 μ M paxilline to block BK channels.

2.3 Immunocytochemistry

Cells were labeled with antibodies as previously described [3]. Briefly, cells were cultured and fixed. Cells were then blocked with normal donkey serum. Primary antibodies were used at 1:250 and included rabbit anti-TRPC1 (ACC-010 polyclonal; Alomone, Jerusalem, Israel), goat anti-Caveolin 1 (ab36152 polyclonal; Abcam, Cambridge, MA), and mouse anti-CIC-3 (clone N258/5 monoclonal; UC Davis/NIH Neuromab Facility, Davis, CA). Secondary antibodies were purchased from Invitrogen, used at 1:500, and included donkey anti-rabbit Alexa 647, donkey anti-mouse Alexa 488, and donkey anti-goat Alexa 546. Confocal imaging was performed as previously described [9] with a 60X water objective. Colocalization was quantified using the Olympus FluoView software package. Total colocalization for all cells in a field-of-view was measured using the Pearson's correlation coefficient and the Mander's overlap coefficient.

2.4 Western Blot

Western blotting was performed as previously described [3] using the following primary antibodies: rabbit anti-TRPC1 (ACC-010 polyclonal; Alomone, Jerusalem, Israel) and mouse anti-glyceraldehyde-3-phosphate dehydrogenase (Abcam, Cambridge, MA).

2.5 Inducible TRPC1 knockdown

Human D54 glioma cells were transfected with non-targeting (NT) or TRPC1 shRNA plasmids as previously described [8].

2.6 Migration Assay

Migration assays were performed as previously described [3]. Cells were incubated in doxycycline prior to the experiments, and not while migration was occurring.

2.7 Data Analysis

Current responses to voltage steps were quantified using Clampfit 8 software (Molecular Devices, Sunnyvale, CA). Raw data were compiled and graphed in Origin 7.5 (MicroCal, Northampton, MA) or Microsoft Excel. Statistical analyses were performed using GaphPad Instat (GraphPad software). One-way ANOVA or t-test was used to determine the p-value as appropriate. All data are reported as mean \pm standard error (* $p < 0.05$).

3. Results

3.1 $[Ca^{2+}]_i$ regulates Cl^- currents in human glioma cells

Previous studies demonstrate that human glioma cells express voltage-gated Cl^- channels, which modulate cellular volume to promote cell motility [1;3;10]. Given that a subset of these Cl^- channels are regulated by Ca^{2+} -sensitive kinases [3;11], we hypothesize that $[Ca^{2+}]_i$ may also regulate Cl^- channel activity. To test this hypothesis, we first performed whole-cell patch clamp experiments on human glioma cells. By manipulating the $[Ca^{2+}]_i$ of the pipette solution, we changed $[Ca^{2+}]_i$ in glioma cells to either 0 nM, 65 nM, or 180 nM. These values were selected, because the resting $[Ca^{2+}]_i$ in glioma cells is about 65 nM [12], and 0 nM and 180 nM represent low and high $[Ca^{2+}]_i$, respectively. After dialyzing cells with the various $[Ca^{2+}]_i$, we stepped cells from -100 to $+120$ mV in 20 mV increments and measured the current responses. We then washed on 200 μ M NPPB to block Cl^- channels. These experiments were performed in the presence of 10 μ M TRAM-34 to eliminate off-target effects of NPPB on Ca^{2+} -activated K^+ channels [13]. NPPB-sensitive Cl^- currents were largest when $[Ca^{2+}]_i = 180$ nM, and smallest when $[Ca^{2+}]_i = 0$ nM (Figure 1A). The NPPB-sensitive Cl^- currents activated by increases in $[Ca^{2+}]_i$ showed time- and voltage-dependent inactivation, matching the electrophysiological properties of CIC-3, a voltage-gated Cl^- channel/transporter highly expressed by glioma cells [5;14–16]. The Ca^{2+} -activated Cl^- currents reversed at 0 mV, as predicted by the Nernst equilibrium potential with symmetric $[Cl^-]$ inside and outside the cells (Figure 1B). At -40 mV, the approximate resting potential of glioma cells [5], increasing $[Ca^{2+}]_i$ from 0 nM to 65 nM significantly increased NPPB-sensitive Cl^- current density from -0.93 ± 0.27 to -1.95 ± 0.32 pA/pF (Figure 1C; $p < 0.05$; $n = 13$ for each group). Further increasing $[Ca^{2+}]_i$ to 180 nM increased current density to -5.18 ± 1.67 pA/pF (Figure 1C; $p < 0.05$). These data indicate that small physiologically relevant changes in $[Ca^{2+}]_i$ regulate Cl^- channel activity in human glioma cells.

3.2 CIC-3 and TRPC1 colocalize to caveolar lipid rafts

Given that increases in $[Ca^{2+}]_i$ activated Cl^- currents that matched the electrophysiological characteristics of CIC-3, we asked what physiological sources of Ca^{2+} might activate CIC-3 to increase Cl^- conductance. Spatially, CIC-3 is located on caveolar lipid rafts, as determined by membrane subfractionation and immunocytochemical experiments [17]. We first confirmed that CIC-3 was found on caveolar lipid rafts by culturing human glioma cells and labeling CIC-3 and Caveolin-1, a marker of caveolar lipid rafts. CIC-3 and Caveolin-1 strongly colocalized, as assessed by confocal imaging, especially on the processes of glioma cells (arrows in Figure 2A–C). To quantify colocalization, we calculated the Pearson's correlation coefficient, which is independent of background intensity and the intensity of overlapping pixels. The Pearson's correlation coefficient between CIC-3 and Caveolin-1 was 0.9 ± 0.03 , indicating a high degree of colocalization. We also calculated the Mander's overlap coefficient, which is sensitive to differences in background intensity, but not sensitive to the differences in the intensity of overlapping pixels. The Mander's overlap coefficient between CIC-3 and Caveolin-1 was 0.9 ± 0.03 , also indicating a high degree of colocalization. CIC-3 also exhibited punctate staining throughout the cell, characteristic of proteins highly expressed on vesicles (Figure 2B–C). Since CIC-3 is located on caveolar lipid rafts, we searched for regulators of $[Ca^{2+}]_i$ that are located in similar subcellular domains. Interestingly, a recent study indicated that transient receptor potential canonical 1 (TRPC1) channels are also located on caveolar lipid rafts in glioma cells [8]. TRPC channels are non-selective cation channels and play an important role in store-operated Ca^{2+} entry to regulate intracellular Ca^{2+} dynamics. Therefore, we asked if CIC-3 and TRPC1 channels were located in similar subcellular domains to understand if Ca^{2+} influx through TRPC1 might affect Cl^- channel activity. As seen in a field-of-view and digital zooms of individual

cells, Caveolin-1, CIC-3, and TRPC1 colocalized on the processes of glioma cells (Figure 2A–C). The Pearson's correlation coefficient was 0.92 ± 0.02 for TRPC1 and CIC-3 and 0.88 ± 0.02 for TRPC1 and Caveolin-1, indicating a high degree of colocalization. The Mander's overlap coefficient was 0.93 ± 0.01 for TRPC1 and CIC-3 and 0.9 ± 0.02 for TRPC1 and Caveolin-1, also indicating a high degree of colocalization. Thus TRPC1 channels appear to be in a privileged spatial domain to regulate Cl^- channel activity via Ca^{2+} .

3.3 TRPC1 knockdown inhibits glioma Cl^- currents

Since there are no specific pharmacological inhibitors of TRPC1, we transfected glioma cells with inducibly-expressed TRPC1 shRNA or inducibly-expressed non-targeting (NT) shRNA to study its potential role in regulating Cl^- currents. Stable TRPC1 protein knockdown was achieved after 5 days of doxycycline treatment in cells transfected with TRPC1 shRNA, but not NT shRNA, as seen in a representative Western blot (Figure 3A). The multiple bands depicted correspond to TRPC1 protein, as they were sensitive to TRPC1 shRNA-mediated protein knockdown. On average band intensity shifted from 1.19 ± 0.5 (arbitrary units) in NT shRNA transfected cells to 0.58 ± 0.12 in TRPC1 shRNA-transfected cells, as normalized to the doxycycline-free condition. We confirmed that this led to a functional loss of TRPC1 by patching onto glioma cells and measuring 2-aminoethoxydiphenyl borate (2-APB)-sensitive currents. 2-APB inhibits TRP channels [18] and blocks TRPC currents in glioma cells [6]. Doxycycline application to NT shRNA-transfected cells did not produce any measurable change in 2-APB-sensitive currents (Figure 3B–C). In these cells at +40 mV, current density did not significantly change upon application of doxycycline (3.4 ± 1.2 to 2.3 ± 0.88 pA/pF; $p > 0.05$; Figure 3C). However, doxycycline application to TRPC1 shRNA-transfected cells significantly inhibited 2-APB-sensitive TRPC1 currents (Figure 3B,D). 2-APB-sensitive current density was significantly reduced from 4.1 ± 1.5 to 0.6 ± 0.6 pA/pF at +40 mV ($p < 0.05$; Figure 3D).

After creating an inducible TRPC1 knockdown, the next step was to assess the potential activation of glioma Cl^- currents by TRPC1 through a Ca^{2+} -dependent mechanism. Because whole-cell patch clamping requires dialysis of the cytoplasmic space with the pipette solution, we employed an amphotericin B perforated-patch approach to measure the effects of TRPC1-mediated Ca^{2+} influx on Cl^- channel activity. Amphotericin B permeabilizes the plasma membrane to monovalent cations and anions, including K^+ , Na^+ , H^+ , and Cl^- , but not divalent cations like Ca^{2+} . This allows electrical access to the cell while leaving the cytoplasmic $[\text{Ca}^{2+}]_i$ unperturbed. To verify that we were in the perforated-patch configuration, we loaded Alexa Fluor 488 hydrazide salt into the pipette solution, and ensured that it did not fill the cell (Figure 4A). After obtaining perforated patches, we stepped glioma cells from -100 to $+120$ mV in 20 mV increments, and then washed on NPPB to block Cl^- channels. Doxycycline treatment of NT shRNA-transfected cells did not produce any appreciable change in NPPB-sensitive currents at +40 mV (2.6 ± 1.2 to 3.7 ± 1.2 pA/pF; $p > 0.05$; Figure 4C). However, doxycycline treatment of TRPC1 shRNA cells inhibited NPPB-sensitive current density from 5.5 ± 1.2 to 1.6 ± 0.4 pA/pF ($p < 0.05$; Figure 4B,D). These data indicate that TRPC1 modulates Cl^- currents in glioma cells. Given our data demonstrating that elevations in $[\text{Ca}^{2+}]_i$ increase Cl^- currents, we hypothesized that TRPC1-mediated Ca^{2+} influx activated Cl^- channels. To test this hypothesis, we performed whole-cell patch clamp experiments of NT shRNA- and TRPC1 shRNA-transfected cells, and clamped $[\text{Ca}^{2+}]_i$ at a very low concentration namely 3 nM using 10 mM EGTA and 0.2 mM CaCl_2 . Even when TRPC1 expression was decreased with application of doxycycline, there was no change in NPPB-sensitive Cl^- currents when $[\text{Ca}^{2+}]_i$ was clamped at 3 nM (Figure 5). Therefore TRPC1-mediated Ca^{2+} influx activates Cl^- currents in human glioma cells.

3.4 TRPC1 and Cl⁻ channels facilitate glioma cell migration

TRPC1 channels are functionally important for glioma pathogenesis. By responding to epidermal growth factor (EGF), TRPC1 channels promote the chemotaxis of migrating cells, spreading cancer burden throughout the brain [8]. We asked if TRPC1 increased migration by activating glioma Cl⁻ channels, which facilitate the shape and volume changes typical of migrating cells [1;19]. To answer this question, we seeded glioma cells on a membrane with 8 μm pores. We then put 10 ng/mL EGF on the bottom of the filter and counted the number of cells migrating through the pores. As previously reported [8], knockdown of TRPC1 expression after doxycycline application significantly decreased EGF-induced chemotaxis (70±11 to 41±6 cells; $p < 0.05$; Figure 6A–B). Additionally, Cl⁻ channel inhibition with NPPB significantly decreased glioma cell chemotaxis from 70±11 to 16±3 cells ($p < 0.05$; Figure 6A–B). To rule out off-target effects of NPPB on Ca²⁺-activated K⁺ channels [13], we performed migration assays in the presence of TRAM-34, a blocker of IK channels. Even after TRAM-34 addition, NPPB decreased glioma cell migration from 62±8 to 16±3 % of control ($p < 0.05$; $n = 5$), demonstrating that NPPB acts at Cl⁻ channels to decrease migration. There was no significant additive effect of TRPC1 knockdown and Cl⁻ channel inhibition, suggesting that TRPC1 and Cl⁻ channels are on the same signaling pathway (Figure 6B). These data indicate that EGF-stimulated migration activates TRPC1, and the following Ca²⁺ influx activates Cl⁻ channels.

4. Discussion

To our knowledge, this is the first demonstration that increases in [Ca²⁺]_i leads to enhanced Cl⁻ channel activity in gliomas (Figure 1). As previously reported, Cl⁻ channels play an important role in the shape and volume changes associated with migrating cells [1;19]. This led us to ask how Cl⁻ channels are physiologically regulated in human glioma cells. We found that knockdown of TRPC1 decreased Cl⁻ conductance in a Ca²⁺-dependent manner. These currents were likely mediated by CIC-3, a voltage-gated Cl⁻ channel/transporter, which are regulated by CaMKII and colocalizes with TRPC1 on caveolar lipid rafts. This interaction of TRPC1 and Cl⁻ channels is functionally important, as inhibition of either decreased EGF-induced chemotaxis of human glioma cells.

4.1 Molecular identity of the glioma Ca²⁺-activated Cl⁻ current

We observed that increases in [Ca²⁺]_i led to larger NPPB-sensitive Cl⁻ currents (Figure 1). However, we did not investigate the molecular identity of the Cl⁻ channel responsible for this. As most Cl⁻ channel inhibitors are non-specific [20], the identities of the Cl⁻ channels can only be discerned through genetic manipulation. Based on previous studies, a likely candidate channel is CIC-3, which is activated by CaMKII, a Ca²⁺-sensitive kinase [21]. Human glioma cells express both CIC-3 and CaMKII, and this CaMKII co-immunoprecipitates with CIC-3 [3]. Because CaMKII forms a physical linkage with CIC-3, which is expressed on the plasma membrane, the interaction of these proteins persists even in dialyzed cells. CaMKII phosphorylation of CIC-3 increases Cl⁻ currents in both growth phase and dividing glioma cells, and this regulation can be blocked with specific CaMKII inhibitors, including autocalmitide-2 related inhibitory peptide (AIP) [3]. Specifically, CaMKII phosphorylates the S109 residue of CIC-3, as demonstrated in in tsA cells, a type of human embryonic kidney cell [15]. When S109 was mutated to an alanine residue, CaMKII no longer activated CIC-3 Cl⁻ currents [15]. These data indicate that increases in [Ca²⁺]_i, which could occur TRPC1-mediated Ca²⁺ influx, may activate CaMKII and CIC-3.

Both TRPC1 and CIC-3 are expressed in glioblastoma patient tissue, indicating that the proposed mechanism may be preserved in human disease. TRPC1 is expressed in several glioma cell lines, including D54, D65, GBM62, STTG1, U87, and U251 [6]. TRPC1 is also

expressed in Grade IV malignant glioma patient tissue [6], where its expression inversely correlates with large multinucleated cells [7]. CIC-3 is expressed in Grade II, II, and IV malignant glioma patient tissue [3]. Interestingly, CIC-3 expression is over-expressed in Grade IV glioblastoma tissue, which correlates with the enhanced invasiveness of glioblastoma cells [3].

Beyond the CIC family of Cl^- channels, a group of Ca^{2+} -activated Cl^- channels (CaCC) may also participate in the Ca^{2+} -dependent Cl^- conductance. The molecular identities of CaCCs are recently becoming identified, and include CLCAs, anoctamins, and bestrophins. The CLCA family requires extremely high, and non-physiological, concentrations of $[\text{Ca}^{2+}]_i$ to become activated [22]. Given our increase in Cl^- conductance with physiological $[\text{Ca}^{2+}]_i$, CLCAs are not likely to be activated by TRPC1 in glioma cells. In contrast, anoctamins are activated by physiological $[\text{Ca}^{2+}]_i$ and are upregulated in several cancers [23]. Additionally, bestrophins are activated by increases in $[\text{Ca}^{2+}]_i$ and can interact with stromal interacting molecule 1 (STIM1), which is the Ca^{2+} -sensor of the endoplasmic reticulum, to increase intracellular Ca^{2+} spikes [24]. This is especially interesting given that TRPC1 and STIM1 also interact to replenish intracellular Ca^{2+} stores [25]. The expression of the anoctamin and bestrophin families in gliomas has not been investigated and warrants further study.

4.2 A mechanistic role for Cl^- channels in TRPC1-induced chemotaxis

Understanding the downstream targets of TRPC1-mediated Ca^{2+} influx, such as Cl^- channels, is important because TRPC1 increases cell migration in several cell types. In glioma cells, TRPC1 localizes to the leading edge on caveolar lipid rafts and promotes chemotactic migration towards EGF [8]. In pancreatic cancer cells, transforming growth factor- β (TGF- β) activates TRPC1 to increase $[\text{Ca}^{2+}]_i$ and migration [26]. Additionally, TRPC1 in renal epithelial cells dictates directionality in migrating cells [27].

How may TRPC1 mechanistically enhance chemotaxis? Our data indicate that Cl^- channels are important downstream targets. TRPC1 could lead to Cl^- channel activation via membrane depolarization or Ca^{2+} influx, and our data indicate that a Ca^{2+} -dependent mechanism is predominant. TRPC1-induced Cl^- channel activation is important, because it may facilitate the shape and volume changes associated with migrating cells. Because Cl^- ions are osmolytes, Cl^- movement across the plasma membrane osmotically draws water across the membrane, changing cell shape and volume [1]. These hydrodynamic changes require the movement of ions through channels or transporters, and TRPC1-induced Cl^- channel activation may be integral to this process. Migrating cells undergo significant volume and shape changes, and if these processes are inhibited by Cl^- channel inhibition, cell migration is impaired [19]. EGF is a known activator of glioma TRPC1 channels [8], and our data indicate that EGF-induced TRPC1 activation may lead to downstream Cl^- channel activation to promote the shape and volume changes typical of migrating cells.

Beyond EGF-induced activation of TRPC1, several ligands that increase $[\text{Ca}^{2+}]_i$ also increase glioma cell migration by facilitating shape and volume changes. For example, bradykinin-induced increases in $[\text{Ca}^{2+}]_i$ can lead to cellular shape changes in migrating cells [28]. Additionally, activation of Ca^{2+} -permeable AMPA receptors can lead to increases in $[\text{Ca}^{2+}]_i$ and promote migration through narrow spaces necessitating robust volume changes [19;29]. Hence, ligand-mediated increases in $[\text{Ca}^{2+}]_i$ may be a conserved mechanism that leads to downstream Cl^- channel activation, leading to the shape and volume changes typical of migrating cells. While our findings explore TRPC1-mediated Cl^- channel activation in human glioma cells, these results may also be applicable to other cell types. Ca^{2+} influx through TRPC1 activating Cl^- channels may be a conserved mechanism by which migrating cells regulate the shape and volume changes necessary for motility.

4.3 TRP and Cl⁻ channels interact in several other cells types

TRPC1 expressed by human glioma cells plays a role in store-operated Ca²⁺ entry, which replenishes intracellular Ca²⁺ stores [7]. Here we demonstrate that these same channels activate endogenous glioma Cl⁻ currents (Figure 3). This mechanism does not appear to be unique to glioma cells, as TRP channels involved in store-operated Ca²⁺ entry in smooth muscle cells also activate a Ca²⁺-dependent Cl⁻ conductance [30;31]. Additionally, others have demonstrated that TRPC1-mediated store-operated Ca²⁺ entry can produce shape changes [32]. Our data suggests that this may occur through activation of Cl⁻ channels, known modulators of cell shape and volume.

In summary, the data presented here demonstrate that TRPC1 activates Cl⁻ channels in human glioma cells. This interaction may be conserved among several other cells types and play an important role in chemotactic migration. Further studies assessing the role of this mechanism in other cell types and discerning the molecular identities of the Ca²⁺-activated Cl⁻ channels are warranted.

Acknowledgments

We thank Dr. Valerie Bomben for creating the inducible cell lines and Dr. Susan L. Campbell for critical reading of the manuscript. We are grateful for the following grants from the National Institutes of Health (National Institute of Neurological Disorders and Stroke): RO1 NS036692 and RO1 NS031234 to H.S. and F31 NS073181 to V.A.C.

References

1. Cuddapah VA, Sontheimer H. Ion Channels and the Control of Cancer Cell Migration. *Am J Physiol Cell Physiol.* 2011; 301:C541–C549. [PubMed: 21543740]
2. Weaver AK, Bomben VC, Sontheimer H. Expression and function of calcium-activated potassium channels in human glioma cells. *Glia.* 2006; 54:223–233. [PubMed: 16817201]
3. Cuddapah VA, Sontheimer H. Molecular interaction and functional regulation of CIC-3 by Ca²⁺/calmodulin-dependent protein kinase II (CaMKII) in human malignant glioma. *J Biol Chem.* 2010; 15:11196.
4. Lakka SS, Rajan M, Gondi C, et al. Adenovirus-mediated expression of antisense MMP-9 in glioma cells inhibits tumor growth and invasion. *Oncogene.* 2002; 21:8011–8019. [PubMed: 12439751]
5. Habela CW, Olsen ML, Sontheimer H. CIC3 is a critical regulator of the cell cycle in normal and malignant glial cells. *J Neurosci.* 2008; 28:9205–9217. [PubMed: 18784301]
6. Bomben VC, Sontheimer HW. Inhibition of transient receptor potential canonical channels impairs cytokinesis in human malignant gliomas. *Cell Prolif.* 2008; 41:98–121. [PubMed: 18211288]
7. Bomben VC, Sontheimer H. Disruption of Transient Receptor Potential Canonical Channel-1 causes incomplete cytokinesis and slows the growth of human malignant gliomas. *Glia.* 2010 in press.
8. Bomben VC, Turner KL, Barclay TT, Sontheimer H. Transient receptor potential canonical channels are essential for chemotactic migration of human malignant gliomas. *J Cell Physiol.* 2011; 226:1879–1888. [PubMed: 21506118]
9. Haas BR, Cuddapah VA, Watkins S, Rohn KJ, Dy TE, Sontheimer H. With-No-Lysine Kinase 3 (Wnk3) stimulates glioma invasion by regulating cell volume. *Am J Physiol Cell Physiol.* 2011; 301:C1150–C1160. [PubMed: 21813709]
10. Lui VC, Lung SS, Pu JK, Hung KN, Leung GK. Invasion of human glioma cells is regulated by multiple chloride channels including CIC-3. *Anticancer Res.* 2010; 30:4515–4524. [PubMed: 21115901]
11. Cuddapah VA, Habela CW, Watkins S, Moore LS, Barclay TT, Sontheimer H. Kinase activation of CIC-3 accelerates cytoplasmic condensation during mitotic cell rounding. *Am J Physiol Cell Physiol.* 2011; 302:C527–C538. [PubMed: 22049206]
12. Manning TJ Jr, Parker JC, Sontheimer H. Role of lysophosphatidic acid and Rho in glioma cell motility. *Cell Motil Cytoskeleton.* 2000; 45:185–199. [PubMed: 10706774]

13. Fioretti B, Castigli E, Calzuola I, Harper AA, Franciolini F, Catacuzzeno L. NPPB block of the intermediate-conductance Ca^{2+} -activated K^{+} channel. *Eur J Pharmacol.* 2004; 497:1–6. [PubMed: 15321728]
14. Olsen ML, Schade S, Lyons SA, Amarillo MD, Sontheimer H. Expression of voltage-gated chloride channels in human glioma cells. *J Neurosci.* 2003; 23:5572–5582. [PubMed: 12843258]
15. Robinson NC, Huang P, Kaetzel MA, Lamb FS, Nelson DJ. Identification of an N-terminal amino acid of the CLC-3 chloride channel critical in phosphorylation-dependent activation of a CaMKII -activated chloride current. *J Physiol.* 2004; 556:353–368. [PubMed: 14754994]
16. Shimada K, Li X, Xu G, Nowak DE, Showalter LA, Weinman SA. Expression and canalicular localization of two isoforms of the *clc-3* chloride channel from rat hepatocytes. *Am J Physiol Gastrointest Liver Physiol* 2000 Aug;279(2):G268–76. 2000; 279:G268–G276.
17. McFerrin MB, Sontheimer H. A role for ion channels in glioma cell invasion. *Neuron Glial Biology.* 2005; 2:39–49.
18. Xu SZ, Zeng F, Boulay G, Grimm C, Harteneck C, Beech DJ. Block of TRPC5 channels by 2-aminoethoxydiphenyl borate: a differential, extracellular and voltage-dependent effect. *Br J Pharmacol.* 2005; 145:405–414. [PubMed: 15806115]
19. Watkins S, Sontheimer H. Hydrodynamic cellular volume changes enable glioma cell invasion. *J Neurosci.* 2011; 31:17250–17259. [PubMed: 22114291]
20. Jentsch TJ, Stein V, Weinreich F, Zdebik AA. Molecular structure and physiological function of chloride channels. *Physiol Rev.* 2002; 82:503–568. [PubMed: 11917096]
21. Huang P, Liu J, Di A, et al. Regulation of human CLC-3 channels by multifunctional Ca^{2+} /calmodulin-dependent protein kinase. *J Biol Chem.* 2001; 276:20093–20100. [PubMed: 11274166]
22. Nilius B, Droogmans G. Amazing chloride channels: an overview. *Acta Physiol Scand.* 2003; 177:119–147. [PubMed: 12558550]
23. Galindo BE, Vacquier VD. Phylogeny of the TMEM16 protein family: some members are overexpressed in cancer. *Int J Mol Med.* 2005; 16:919–924. [PubMed: 16211264]
24. Barro-Soria R, Aldehni F, Almaca J, Witzgall R, Schreiber R, Kunzelmann K. ER-localized bestrophin 1 activates Ca^{2+} -dependent ion channels TMEM16A and SK4 possibly by acting as a counterion channel. *Pflugers Arch.* 2010; 459:485–497. [PubMed: 19823864]
25. Lopez JJ, Salido GM, Pariente JA, Rosado JA. Interaction of STIM1 with endogenously expressed human canonical TRP1 upon depletion of intracellular Ca^{2+} stores. *J Biol Chem.* 2006; 281:28254–28264. [PubMed: 16870612]
26. Dong H, Shim KN, Li JM, et al. Molecular mechanisms underlying Ca^{2+} -mediated motility of human pancreatic duct cells. *Am J Physiol Cell Physiol.* 2010; 299:C1493–C1503. [PubMed: 20861471]
27. Fabian A, Fortmann T, Dieterich P, et al. TRPC1 channels regulate directionality of migrating cells. *Pflugers Arch.* 2008; 457:475–484. [PubMed: 18542994]
28. Montana V, Sontheimer H. Bradykinin Promotes the Chemotactic Invasion of Primary Brain Tumors. *The Journal of Neuroscience.* 2011; 31:4858–4867. [PubMed: 21451024]
29. Lyons SA, Chung WJ, Weaver AK, Ogunrinu T, Sontheimer H. Autocrine glutamate signaling promotes glioma cell invasion. *Cancer Res.* 2007; 67:9463–9471. [PubMed: 17909056]
30. Angermann JE, Forrest AS, Greenwood IA, Leblanc N. Activation of Ca^{2+} -activated Cl^{-} channels by store-operated Ca^{2+} entry in arterial smooth muscle cells does not require reverse-mode $\text{Na}^{+}/\text{Ca}^{2+}$ exchange. *Can J Physiol Pharmacol.* 2012; 90:903–921. [PubMed: 22734601]
31. Forrest AS, Angermann JE, Raghunathan R, Lachendro C, Greenwood IA, Leblanc N. Intricate interaction between store-operated calcium entry and calcium-activated chloride channels in pulmonary artery smooth muscle cells. *Adv Exp Med Biol.* 2010; 661:31–55. 31–55. [PubMed: 20204722]
32. Moore TM, Brough GH, Babal P, Kelly JJ, Li M, Stevens T. Store-operated calcium entry promotes shape change in pulmonary endothelial cells expressing *Trp1*. *Am J Physiol.* 1998; 275:L574–L582. [PubMed: 9728053]

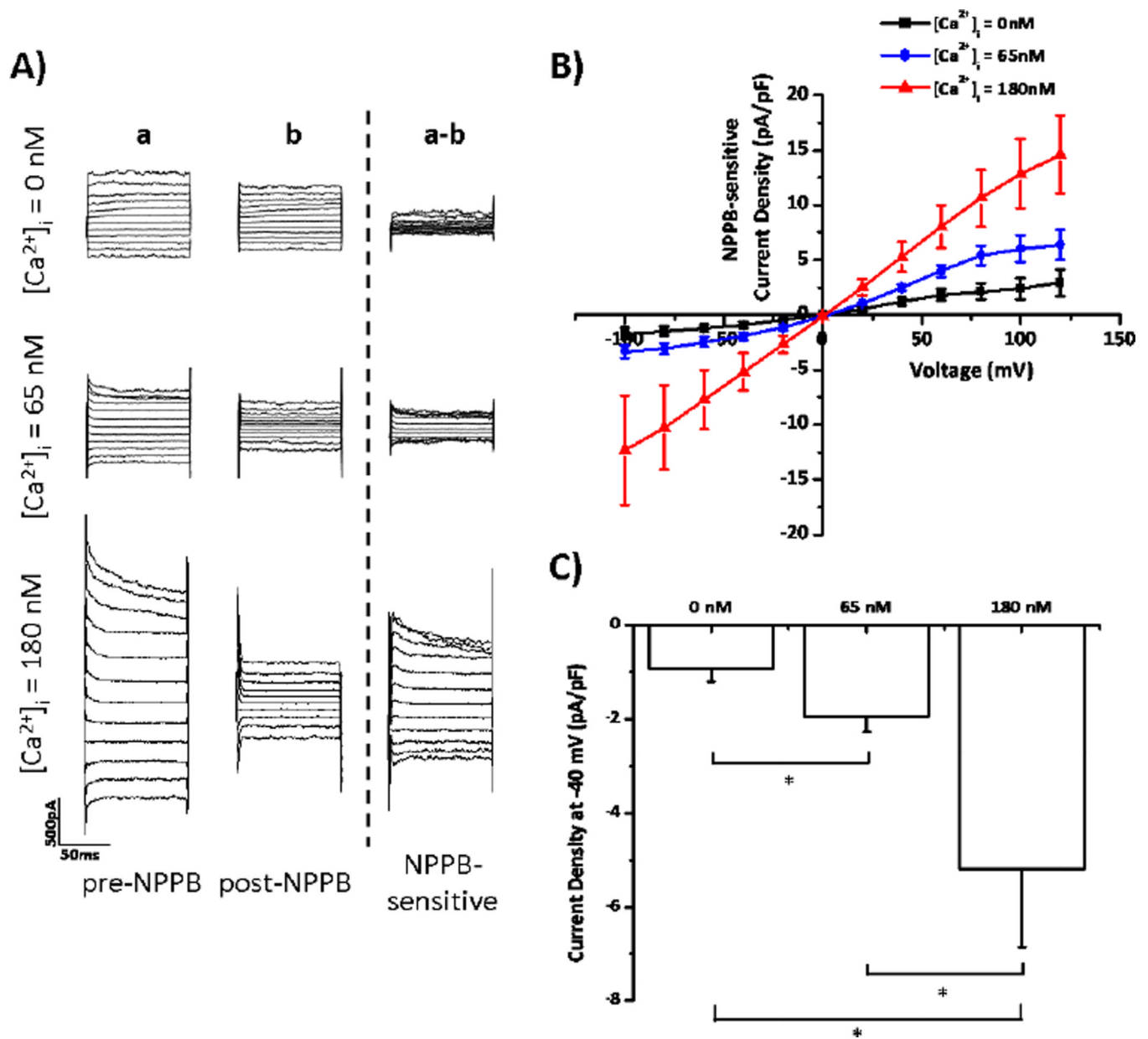


Figure 1. Increases in $[Ca^{2+}]_i$ activate glioma Cl^- currents

Glioma cells were held at -40 mV and then stepped from -100 mV to $+120$ mV in 20 mV increments. A) Representative traces at $[Ca^{2+}]_i = 0$, 65 , or 180 nM. Column (a) is pre-NPPB current. Column (b) is post-NPPB current. Column (a-b) is NPPB-sensitive current. B) NPPB-sensitive current-versus-voltage relationships at various $[Ca^{2+}]_i$. C) Current density at -40 mV. * $p < 0.05$. $n = 13$ for each group.

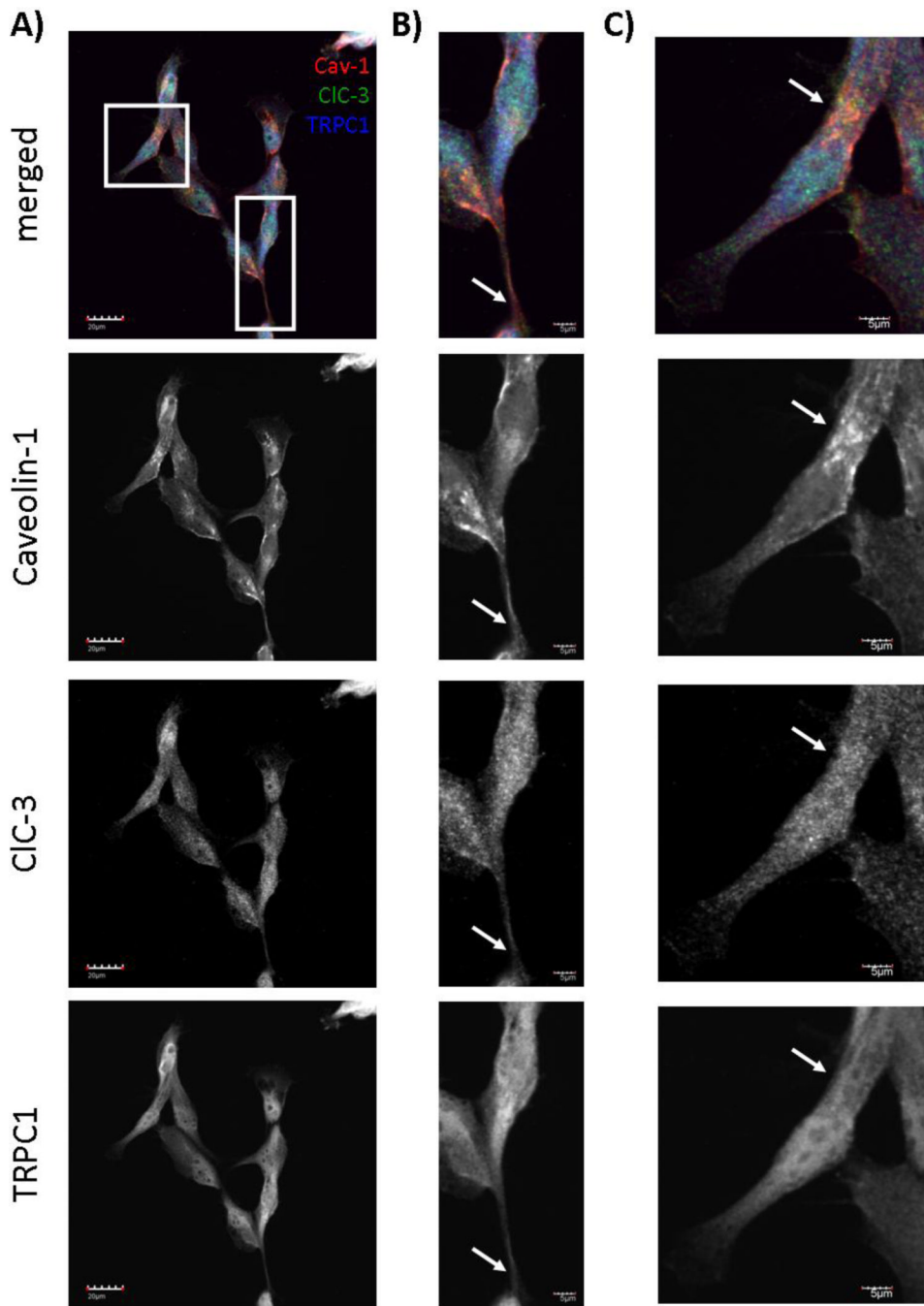


Figure 2. CIC-3 and TRPC1 colocalize on caveolar lipid rafts

Confocal imaging of cultured D54 human glioma cells reveals overlap of CIC-3, TRPC1, and Caveolin-1 signals. Caveolin-1 is labeled in red. CIC-3 is labeled in green. TRPC1 is labeled in blue. A) Field-of-view of cultured human glioma cells. Scale bar = 20 μm . B) and C) Digital zooms of individual cells boxed in A). Scale bar = 5 μm . z-axis = 1.75 μm for all images.

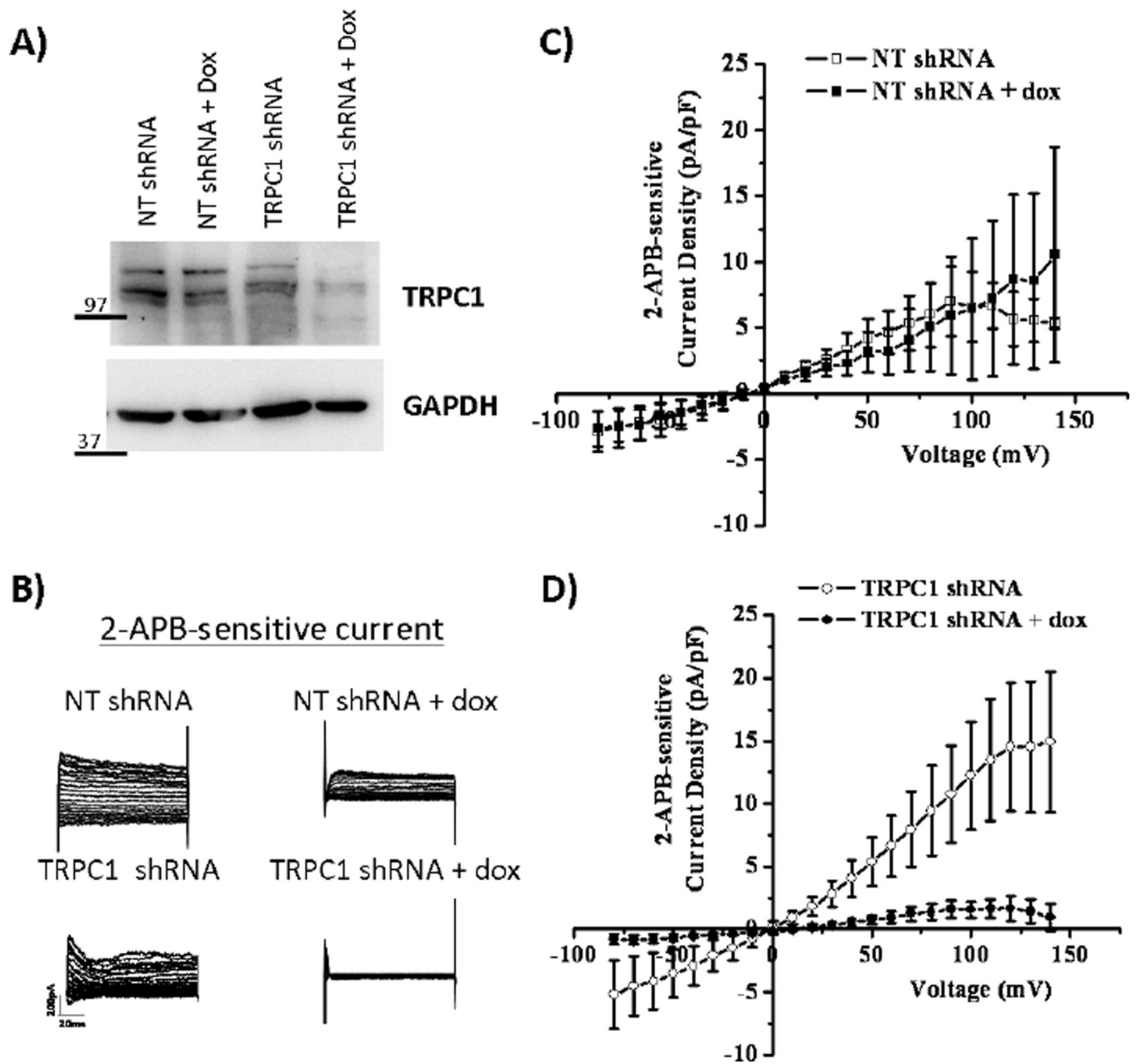


Figure 3. Verification of inducible TRPC1 knockdown in human glioma cells

A) Application of doxycycline for 5 days inhibits endogenous TRPC1 protein expression in human glioma cells transfected with TRPC1 shRNA but not NT shRNA. GAPDH is depicted as a loading control. B) Glioma cells were held at -40 mV and subsequently stepped from -80 mV to $+140$ mV in 10 mV increments. Representative traces of 2-APB-sensitive current are depicted for each group. TRPC1 knockdown leads to a loss of 2-APB-sensitive current. C) and D) 2-APB-sensitive current-versus-voltage relationships are depicted for NT shRNA- and TRPC1 shRNA-transfected cells. $n = 3-6$ for each group.

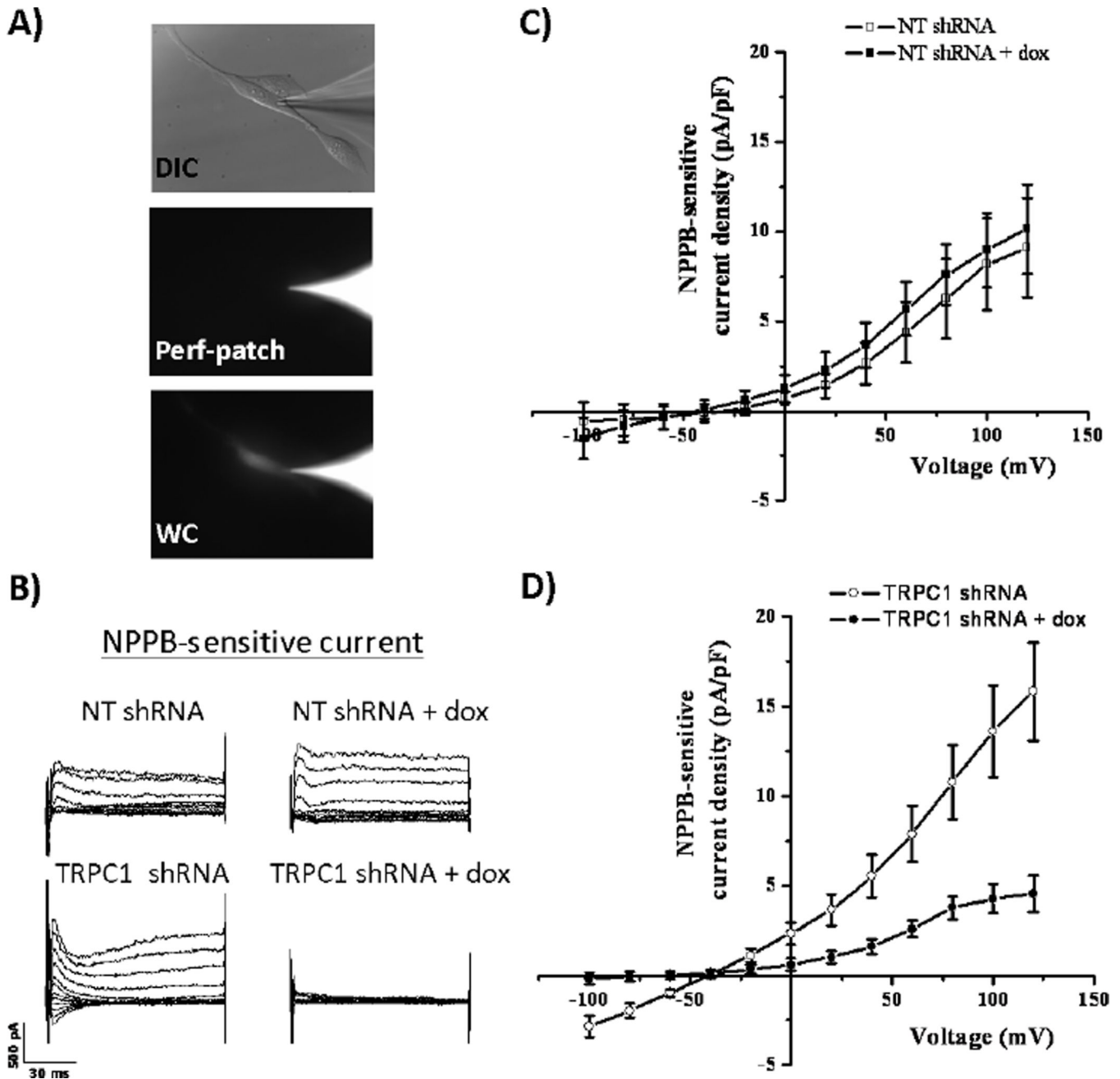
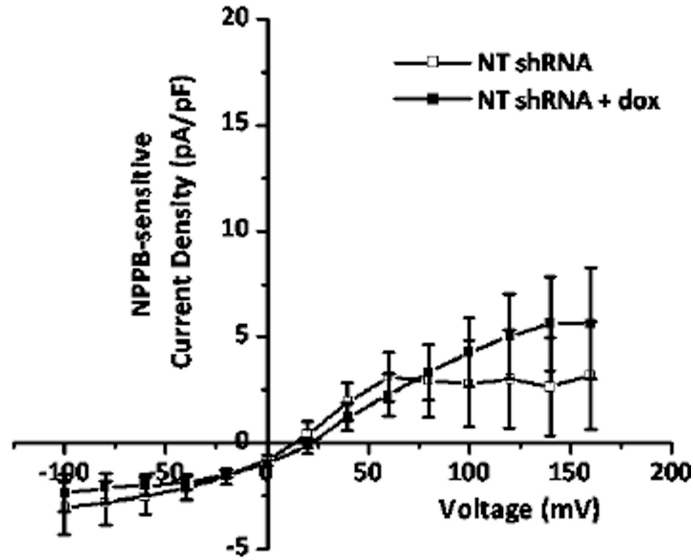


Figure 4. TRPC1 knockdown inhibits NPPB-sensitive Cl⁻ currents

A) Top panel shows representative glioma cell with pipette tip in differential interference contrast microscopy (DIC). For the same cell, middle panel show Alexa 488 fluorescence in pipette tip, but not cell, verifying the perforated-patch configuration. The bottom panel demonstrates movement of the Alexa 488 signal into the cell in whole-cell configuration. B) Glioma cells were held at -40 mV and subsequently stepped from -100 mV to +120 mV in 20 mV increments. Representative traces of NPPB-sensitive current are depicted for each group. TRPC1 knockdown leads to a loss of NPPB-sensitive current. C) and D) NPPB-sensitive current-versus-voltage relationships are depicted for NT shRNA- and TRPC1 shRNA-transfected cells. n = 9–11 for each group.

A) Nominally Ca^{2+} -free



B) Nominally Ca^{2+} -free

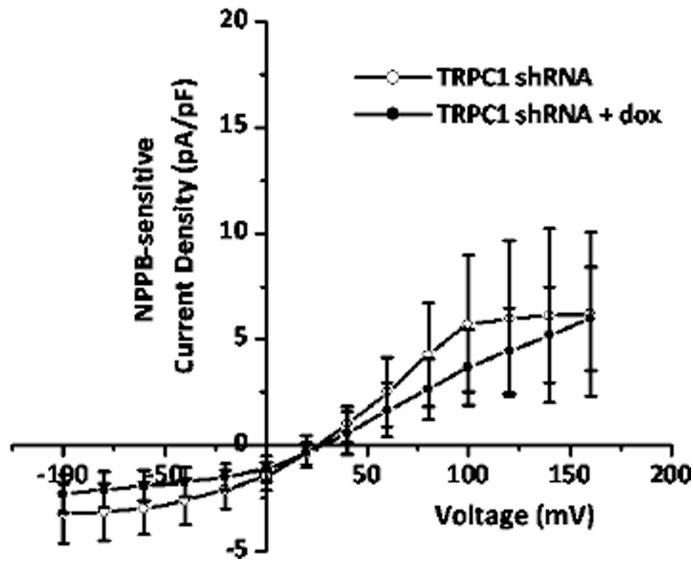
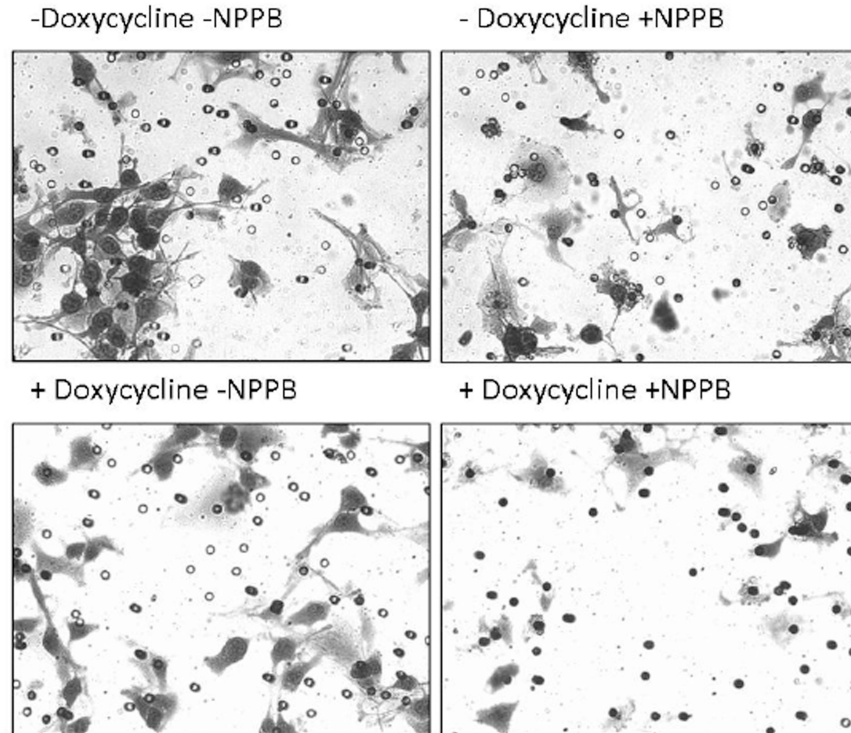
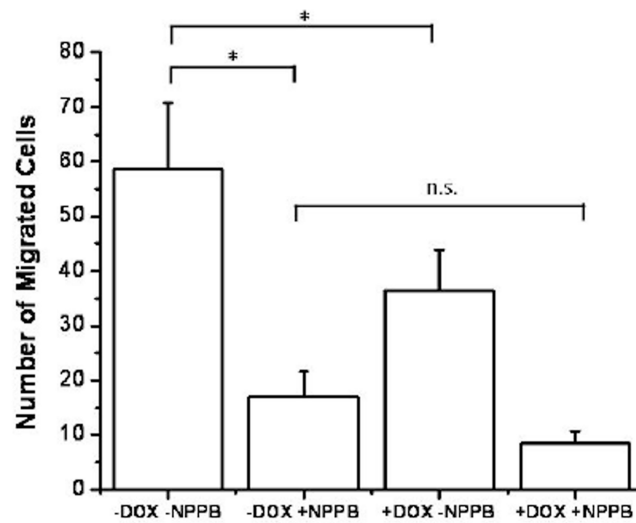


Figure 5. Clamping $[\text{Ca}^{2+}]_i$ at 3nM eliminates TRPC1 modulation of Cl^- currents

A) and B) Glioma cells were held at -40 mV in whole-cell configuration and subsequently stepped from -100 mV to $+160$ mV in 20 mV increments. NPPB-sensitive current-versus-voltage relationships are depicted for NT shRNA- and TRPC1 shRNA-transfected cells. $n = 6-10$ for each group.

A) TRPC1 shRNA**B)****Figure 6. TRPC1 and Cl⁻ channels facilitate glioma migration**

A) Cells transfected with TRPC1 shRNA were exposed to doxycycline and/or NPPB. Representative images of migrated cells through 8µm pores are depicted for each group. B) Mean number of migrated cells for each group. * $p < 0.05$. $n = 7$.